2019 American Control Conference (ACC)
Philadelphia, PA, USA, July 10-12, 2019

Stochastic Modeling and Control of Circulatory System with a Left Ventricular Assist Device*

Jeongeun Son, Dongping Du, and Yuncheng Du, *Member, IEEE*

Abstract— **Left ventricular assist device (LVAD) has been considered as a treatment option for end-stage congestive heart failure to assist an ailing heart to meet the circulatory demand. However, several important issues still challenge the long-term use of the LVAD as a bridge to transplantation or as a destination therapy. Specifically, the development of appropriate feedback controllers to adjust pump speed is crucial. The controller should automatically adjust the pump speed to meet different demands of blood without inducing suction. Suction means that the LVAD seeks to pump out more blood than that is available in the heart, which can collapse the failing heart and result in sudden death. In addition, hemodynamics involves variability due to patients' heterogeneity and stochastic nature of cardiovascular system. The variability poses significant challenges for the control system design of an LVAD. A self-tuning controller is developed in this work, which can adjust the pump speed to meet the physiological demands for different levels of activity, while accounting for variations in hemodynamics. A stochastic state space model will be firstly developed using a generalized polynomial chaos (gPC) expansion, which describes interactions between the LVAD and the cardiovascular system. In addition, the model can further predict the variability in pump flow for a finite future control horizon based on the current available information of pump flow. The prediction of variance is used as a tuning criterion to update the controller gain in a real time manner. The efficiency of the self-tuning control algorithm in this work is validated with two different case scenarios, representing different levels of activity for heart failure patients. The results show that the controller can successfully adjust the pump speed while avoiding suction.**

I. Introduction

Heart transplantation is well recognized as the best therapy for end-stage congestive heart failure (HF) patients [1]. Due to limited donor hearts, however, patients generally wait for a long period of time before finding a match, and approximately 30% of them will die during the waiting of heart transplantation [2]. Mechanical circulatory assist device, i.e., the left ventricular assist device (LVAD), has been used as a treatment option for end-stage HF patients [3]. The goal of LVAD is to assist an ailing heart to meet circulatory demands of patients and provide them with as close to a normal lifestyle as possible before a compatible donor heart is available, or until the ailing heart recovers in some cases [4].

As a bridge to heart transplantation or as a destination therapy, LVAD can benefit HF patients to a greater extent and allow them to return to home and work environment. Patients may experience wide variations in the demands of blood flow as they become more active. To meet the varying physiological activities, LVAD must be able to adjust its speed. An important challenge is the development of appropriate control algorithm to regulate pump speed to meet different circulatory demands. For example, regurgitation may occur if the pump speed is too slow, causing the backflow from the aorta to the left ventricle. Also, suction can happen if the pump speed is too high, which means the LVAD seeks to draw more blood from the ventricle than the available blood in the heart. The control algorithm should avoid these extremes, while tuning the speed to meet the body's demand during different physical activities.

Several control algorithms have been reported to tune pump speed. A gain-scheduling controller was used to regulate pump speed by maintaining the pressure difference between the aorta and the left ventricle [5]. However, such a method cannot assure adequate cardiac output. Using the heart rate, a feedback control strategy was proposed [6], but the strategy cannot prevent suction. A Gaussian process was used to build a model to predict the viscosity for the control of LVAD. However, the accuracy of the model highly depends on the training set and has limited ability for responding to sudden changes in blood demands [7]. It is worth mentioning that all the aforementioned techniques require additional information such as ventricular pressure for control purposes, which is not easy to measure. However, it is reported that pump flow can be easily measured [2] or estimated [8]. Thus, we developed a control algorithm using pump flow data in this work to automatically adjust the pump speed.

The cardiovascular system generally involves a multitude of interacting subsystems and networks. The dynamics often vary between different individuals and within the same patient over time. The inter- and/or intra-patient variability, i.e., uncertainty, poses a significant challenge to develop efficient control algorithms for LVADs. Sampling-based methods such as Monte Carlo (MC) simulations are one of the most popular techniques to deal with such uncertainty. However, MC can be computationally demanding, as it requires many simulations to ensure accurate results. Recently, the generalized polynomial chaos (gPC) expansion has been used in different engineering problems such as control [9], optimization [10], and stochastic modeling [11], which shows the superiority of gPC in terms of computation time.

This paper aims to develop a feedback control algorithm, using information extracted from pump flow, to regulate pump speed, while taking into account uncertainty such as the time varying physical activity of patients. The control strategy can automatically adjust the pump speed to meet the blood demand and avoid the suction. The paper is organized as follows. The

* Research supported by National Science Foundation (CMMI-1646664, CMMI-1728338, and CMMI-1727487).

J. Son and Y. Du are with the Department of Chemical & Biomolecular Engineering, Clarkson University, Potsdam, NY 13699 USA. (Corresponding author phone: +1 315-268-2284, e-mail: ydu@clarkson.edu).

D. Du. is with the Department of Industrial, Manufacturing & Systems Engineering, Texas Tech University, Lubbock, TX 43061 USA. Phone: 806-834-7388. (e-mail: dongping.du@ttu.edu).

nonlinear model of cardiovascular system implanted with a LVAD, and theoretical background of gPC are given in Section II. The control design is presented in Section III, followed by results in Section IV and conclusions in Section V.

II. THEORETICAL BACKGROUND

A. Cardiovascular-Pump Model

Several dynamical models with varying complexity have been previously developed [2, 12, 13]. Following previous work in [2], it is assumed that pulmonary circulation and right ventricle are healthy in this work. Thus, their effect on the LVAD can be neglected. A previous reported circuit model with sixth-order nonlinear time-varying lumped parameters is used to simulate left ventricle hemodynamics and the LVAD, which is described as [2]:

$$\dot{\boldsymbol{x}} = \boldsymbol{A}(t)\boldsymbol{x} + \boldsymbol{P}(t)p(\boldsymbol{x}) + bu(t) \quad (1)$$

$$y = [0 \quad 0 \quad 0 \quad 0 \quad 0 \quad 1]\boldsymbol{x} \quad (2)$$

where $\boldsymbol{x}$ is the states used in the cardiovascular-LVAD model, and y is the measured pump flow. Table I shows the description of each state in $\boldsymbol{x}$. $\boldsymbol{A}(t)$ and $\boldsymbol{P}(t)$ are 6×6 and 6×2 time-varying matrices, b is a 6×1 constant vector, and $p(\boldsymbol{x})$ represents the nonlinear behavior of mitral and aortic values. In addition, $u(t)=\omega^2(t)$ is the control variable, i.e., pump speed $\omega(t)$ that will be tuned to meet the physiological demands. This model was experimentally validated by comparing the hemodynamic waveforms obtained from the model to a patient [2]. The matrices, values of model parameters and their descriptions can be found in [2].

TABLE I. DESCRIPTION OF STATES USED IN THE MODEL [2]

Variables in *[2]*	Definition of variables in *[2]*
x_1	Left ventricular pressure
x_2	Left atrial pressure
x_3	Arterial pressure
x_4	Aortic pressure
x_5	Total blood flow
x_6	LVAD pump flow

For completeness, the model is briefly discussed here. A compliance C_R is used to set the preload pressure in the left atrium. A resistor R_M and a diode D_M are used to describe the mitral valve, while a resistor R_A and a diode D_A are used for the aortic valve. The left ventricle $C(t)$ is approximated with a time-varying compliance and C_A is the aortic compliance. A four-element Windkessel model (R_c, L_s, C_s, and R_s) is used to represent the afterload in [2], where resistor R_s is the systemic vascular resistance (SVR). Physiologically, it varies according to the level of activity, e.g., SVR decreases when patients are exercising and has a larger value when patients are resting. Since the level of activity cannot be known with certainty, it will be assumed as a stochastic variable in this work, which is approximated with a gPC model as discussed later. The dynamic behavior of the left ventricle can be defined by an elastance function $E(t) = 1/C(t)$ as [14, 2]:

$$E(t) = (E_{max} - E_{min})\mathrm{E}'(t') + E_{min} \quad (3)$$

where $\mathrm{E}'(t')$ is the normalized elastance, and E_{max} and E_{min} are the maximum and the minimum value of $E(t)$, respectively. For ailing hearts, a smaller value of E_{max} is often used in the model [2]. Physiologically, it means that the pumping strength of a native failing heart is weaker than a healthy heart.

Resistance R_i and inductor L_i are used to represent the inlet cannula, which is a plastic rigid tube that connects the pump to the heart. The outlet cannula is described by resistance R_o and inductor L_o. A semiempirical model is used to describe the relationship between the pressure difference H across the pump, the pump speed as well as the pump flow as [2]:

$$H = z_0 x_6 + z_1 \frac{dx_6}{dt} + z_2 u^2 \quad (4)$$

where z_0, z_1, and z_2 are LVAD-dependent parameters estimated from experiments [2]. Resistance R_k in the model is a time varying parameter that can define the phenomenon of suction, which can be mathematically described as [2]:

$$R_k = \begin{cases} 0 & \text{if } x_1(t) > x_1^t \\ \vartheta(x_1(t) - x_1^t) & \text{if } x_1(t) \le x_1^t \end{cases} \quad (5)$$

where ϑ and x_1^t are weight and threshold pressure [2].

B. Generalized Polynomial Chaos (gPC) Expansion

The gPC expansion approximates uncertainty as another random variable with *a priori* probability density distribution (PDF) [15]. In this work, R_s (SVR) in (1) is approximated with a gPC model, since it represents the level of activity and can vary over time. It is assumed that R_s consists of stochastic perturbations superimposed on a particular set of mean values. The mean values describe different levels of activity, while the perturbations around each mean value define the intra-patient variability over time. A schematic of different mean values of R_s and corresponding perturbations is shown in Fig. 1.

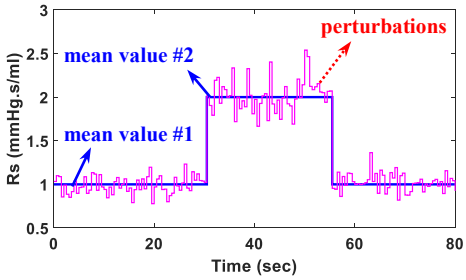

Figure 1. Illustration of time-varying systemic vascular resistance (SVR)

Since the objective is to adjust the pump speed in order to meet the blood demands while avoiding suction, it is useful to evaluate the relationship between stochasticity in R_s and pump flow x_6 as well as other physiological states in (1). First, R_s is approximated with a random variable ξ as [15]:

$$R_s(t, \xi) = \sum_{k=0}^{\infty} \hat{r}_{i,k}(t)\Phi_k(\xi) \approx \sum_{k=0}^{q} \hat{r}_{i,k}(t)\Phi_k(\xi) \quad (6)$$

where ξ is a random variable used to approximate R_s, $\hat{r}_{i,k}$ is the gPC coefficients calculated such that R_s follows *a priori* PDF of R_s, and $\Phi_k(\xi)$ is the polynomial basis functions. Due to uncertainty in R_s, each state in $\boldsymbol{x}$ can be estimated with a set of orthogonal polynomial basis functions $\varphi_l(\xi)$ as [15]:

$$x_j(t,\xi)=\sum_{l=0}^{\infty}\hat{x}_{j,l}(t)\varphi_l(\xi)\approx\sum_{l=0}^{Q}\hat{x}_{j,l}(t)\varphi_l(\xi) \quad (7)$$

where $\hat{x}_{j,l}$ is gPC coefficients calculated with model (1) and a Galerkin projection, which can project (1) onto each one of the polynomial chaos basis functions $\varphi_l(\xi)$ as [15]:

$$\langle \dot{\boldsymbol{x}}, \varphi_l(\xi)\rangle = \langle \boldsymbol{A}(t)\boldsymbol{x} + \boldsymbol{P}(t)p(\boldsymbol{x}) + bu(t), R_s(t,\xi),\varphi_l(\xi)\rangle \quad (8)$$

For practical application, (6) and (7) are often truncated to a finite number of terms, i.e., q and Q. The total number of terms in (7) is approximated as a function of an arbitrary order q in (6) that is necessary to estimate *a priori* PDF of R_s and the number of uncertainty (i.e., n=1 in this work) as [15]:

$$Q+1 = ((n+q!)/(n!q!)) \quad (9)$$

The inner product between two vectors in (8) is defined as:

$$\langle \psi(\xi), \psi'(\xi)\rangle = \int \psi(\xi)\psi'(\xi)W(\xi)\,d\xi \quad (10)$$

where the integral is calculated over the domain defined by ξ, and $W(\xi)$ is the weighting function, i.e., PDF of ξ. Once the coefficients of gPC expansion of $\boldsymbol{x}$ in (7) are available, it is possible to rapidly estimate statistical moments such as the mean and the variance of $\boldsymbol{x}$ at any time interval t as [15]:

$$\begin{aligned} E(x_j(t)) &= E\left(\sum_{l=0}^{Q}\hat{x}_{j,1}(t)\varphi_l\right) \\ &= \hat{x}_{j,0}(t)\,E(\varphi_0)+\sum_{l=1}^{Q}E(\varphi_l) = \hat{x}_{j,0}(t) \end{aligned} \quad (11)$$

$$\begin{aligned} Var(x_j(t)) &= E\left((x(t)-E(x_j(t)))^2\right) \\ &= E\left(\left(\sum_{l=0}^{Q}\hat{x}_{j,l}(t)\varphi_l - \hat{x}_{j,(l=0)}(t)\right)^2\right) \\ &= E\left(\left(\sum_{l=0}^{Q}\hat{x}_{j,l}(t)\varphi_l\right)^2\right) = \sum_{l=0}^{Q}\hat{x}_{j,l}(t)^2\,E(\varphi_l^2) \end{aligned} \quad (12)$$

From (11) and (12), the mean value of $\boldsymbol{x}$ can be calculated with gPC coefficient $\hat{x}_{j,l=0}$, while other higher order statistical moments such as variance can be computed with the other coefficients [15]. The gPC offers a rapid calculation of mean and variance of $\boldsymbol{x}$, which provides important information for the tuning of the controller as discussed below.

III. FEEDBACK CONTROL UNDER UNCERTAINTY

The cardiovascular-pump model has 3 parameters that can change with respect to physiological conditions of patients, i.e., R_s (SVR), heart rate, and the contractility strength of the native heart (E_{max}). In this work, we focus on the changes in R_s, which indicates possible continuous changes in patient's activity. In the presence of uncertainty, the control objective is to adjust an LVAD with respect to different activities to provide the desired cardiac outputs, while avoiding suction.

The only mechanism to regulate the LVAD is to change the pump speed to meet possible time varying blood demands, which requires a reference (or measured variable) to infer the pump operating conditions. Since the current implantable sensing technologies has limited capability to provide accurate measurements of cardiac parameters [2, 5], we use pump flow to decide optimal LVAD speeds. The pump flow can be easily measured by ultrasonic flow transducers that are clamped on the pump cannula [16]. Using the measurements of pump flow, the control design will be explained as below.

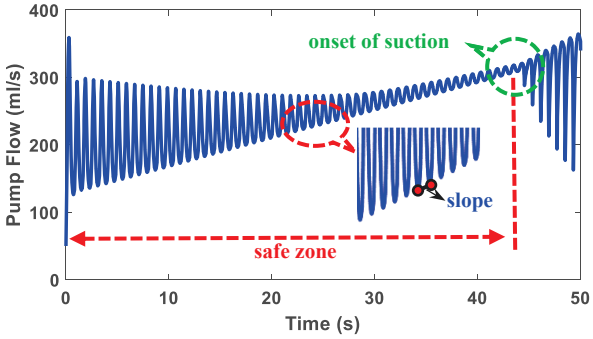

Figure 2. Profile of pump flow of linearly incrased pump speed. In this example, R_s is set to 0.5mmHg·s/ml and the suction occurs when the pump speed is above 1.65×10^4 krpm

For clarity, Fig. 2 shows the pump flow when the pump speed is linearly increased until suction happens. Similar to previously reported works [2, 8, 5], it was found that two signatures are useful to characterize the onset of suction, which includes: (*i*) a significant change between the minimum pump flow in two consecutive cardiac cycles, defined by the slope of a straight line fitted to the minimum pump flow speeds, and (*ii*) a large variation in the flow signal immediately after the occurrence of suction. In this current work, these two signatures will be used to adjust pump speed. Note that the results in Fig. 2 were obtained with deterministic values of R_s and heart rate. The effect of uncertainty in R_s and heart rate on pump flow will be studied in the future due to space limits.

When the pump operates in a safe zone, it is clear from Fig. 2 that the slope defined by two consecutive minimum pump flow measurements is positive. When the speed increases, the slope will decrease and approach zero. When suction occurs, a sudden change in the sign of the slope was observed, i.e., the slope switches from a positive value to a negative value. A sign change in the slope will be used as an indicator to adjust pump speed. Further, the variation in pump flow after the onset of suction can be used as a tuning criterion. As seen in Fig. 2, the pulsatility of pump flow in each cardiac cycle increases when a suction has occurred. Using flow signals and the gPC model, the variance of the pulsatility in pump flow can be rapidly estimated, which will be used to reconfigure the controller.

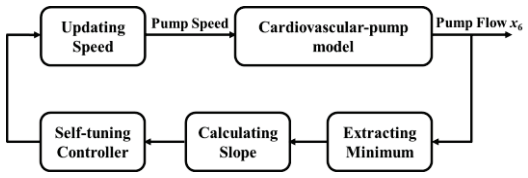

Figure 3. Schematic of the gain-scheduling feedback control of LVAD

Using these signatures, a self-tuning feedback proportional (P) controller is developed in this work. Fig. 3 shows the general block of the feedback control strategy. The update law of the controller is defined as:

$$\omega(t+1) = \omega(t) + K_p \frac{dx_6^m}{dt} \tag{13}$$

where K_p is the controller gain, x_6^m is the minimum pump flow in each cardiac cycle, dx_6^m/dt is the slope of the straight line fitted to two consecutive pump flow measurements, and $\omega(\cdot)$ is the pump speed. The controller gain K_p is defined as:

$$K_p = \begin{cases} c_1 & \text{if } dx_6^m/dt \geq 0 \\ c_1 + \mu\sigma & \text{if } dx_6^m/dt < 0 \end{cases} \tag{14}$$

where c_1 is a fixed controller gain that controls the rate of speed adjustment before suction. The choice of c_1 is patient specific. For example, a smaller value of c_1 can be used for severe HF patients, since it will result in conservative adjustment in pump speed. Once a suction has been identified, the controller gain K_p will be re-adjusted to quickly bring the pump back to a safe operating zone.

The sign change in the slope is a good indicator of suction. However, pump flow signals can be corrupted by measurement noise. To reduce the effect of the measurement noise on suction identification, a time moving window of the pump flow will be used, which involves a few data points of pump flow. The slope is then calculated for every two consecutive data points in the moving window, and then the suction can be determined by examining the constancy between consecutive slopes. Once a suction has been confirmed, the switch between two controller gains as given in (13) will be executed.

Using the gPC model, the mean value and the variance of pump flow can be predicted for each cardiac cycle. Parameter σ in (13) is the time-varying variance calculated with the gPC model. The calculation of σ proceeds as follows.

(*i*) A set of gPC models are generated with each of the mean values of R_s following the procedures descried in Section II. Note that values of R_s decrease during exercising and increase in hypertension, and these values can be calibrated with data or set up by clinicians as *a priori* [17].

(*ii*) At the end of the systole, the gPC coefficients for each state in (1) are stored to generate an offline lookup table, when different mean values of R_s are used.

(*iii*) Using the gPC coefficients of pump flow x_6, a family of PDF profiles can be formulated as shown in Fig. 4. This will be further used to identify a particular mean value of R_s, when the pump flow measurement is available. The PDF profiles are approximated by substituting samples generated in the domain defined by ξ into the gPC model (7) and by a binning algorithm previously reported [18].

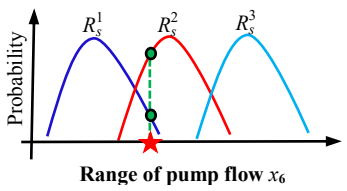

Figure 4. Identification of R_s using the PDF profiles of pump flow

(*iv*) When a measurement of pump flow is available, e.g., the star in Fig. 4, it will be referred to the PDF profiles. The mean value of R_s can be inferred by assessing the probability with respect to each of the PDF profiles. As seen in Fig. 4, two probabilities can be obtained, and R_s^2 can be identified and used to describe the level of activity, as the probability is maximal.

(*v*) The gPC coefficients of the value of R_s will be selected from the lookup table, and further used to predict the gPC coefficients of each state in $\boldsymbol{x}$ based on the current data of the pump flow. For prediction, the mean value of pump flow in the lookup table will be replaced with the latest measurement of flow, while other coefficients remain the same.

(*vi*) Based on these initial values, the gPC model can predict the gPC coefficients of all states in (1) for a finite future control horizon in a real-time manner, from which variance σ of pump flow can be calculated using (12). This will be further used to update the controller gain as shown in (14).

These procedures for adjusting the controller gain will be repeated until the change in σ is found to be within a predefined threshold ε. In addition, constraints of σ are used to control the tuning rate of pump speed to avoid overshoot or suction. It is important to note that a tuning weight μ is used to ensure c_1 and $\mu\sigma$ have the same magnitude to avoid abruptly adjustment in pump speed, which may have deleterious effect on the heart.

IV. RESULTS AND DISCUSSION

The objective of the feedback controller is to adjust pump speed to meet the physiological demands for different physical activities, while maintaining the pump speed lower than a level at which the suction may happen. To evaluate the efficiency, two case scenarios were investigated in this work, which are described in the following sections.

A. Formulation of gPC models

To show how gPC operates and to assess the performance of the feedback controller, three mean values of R_s (SVR) are used, i.e., 0.5 mm Hg/ml/s, 1 mm Hg/ml/s, and 2 mm Hg/ml/s, respectively. The increase in the mean value of R_s indicates a less-active physical activity, e.g., a patient is resting, and vice versa. In order to show time-varying physiological dynamics of patients, a 10% variation around each of these mean values is assumed in this work. Following the procedures in Section II, Fig. 5 shows the hemodynamic waveforms such as left ventricular pressure (LVP, x_1), aortic pressure (AoP, x_4), and aortic flow (AF, x_6), where the mean of R_s is 1 mm Hg/ml/s and a 10% variation is assumed. The heart rate is 75 bpm and the contractility strength of the native heart (E_{max}) is 2 mm Hg/ml. The results were validated by Monte Carlo simulations, but the details are not given due to space limits. For MC and gPC, the mean values were compared to the simulation results obtained with deterministic models and the relative error was calculated. It was found that the relative error of MC and gPC has the same magnitude.

In Fig. 5, the first column shows the gPC coefficients, while the second column shows the mean and the variance calculated with the coefficients. Note that for each mean value of R_s, the gPC coefficients will be stored in a lookup table,

which is further used to predict the hemodynamics over a finite future control horizon. Given the predicted values of each state in (1), the variance of the pump flow can be estimated, which can then be used to adjust the controller gain as explained in Section III.

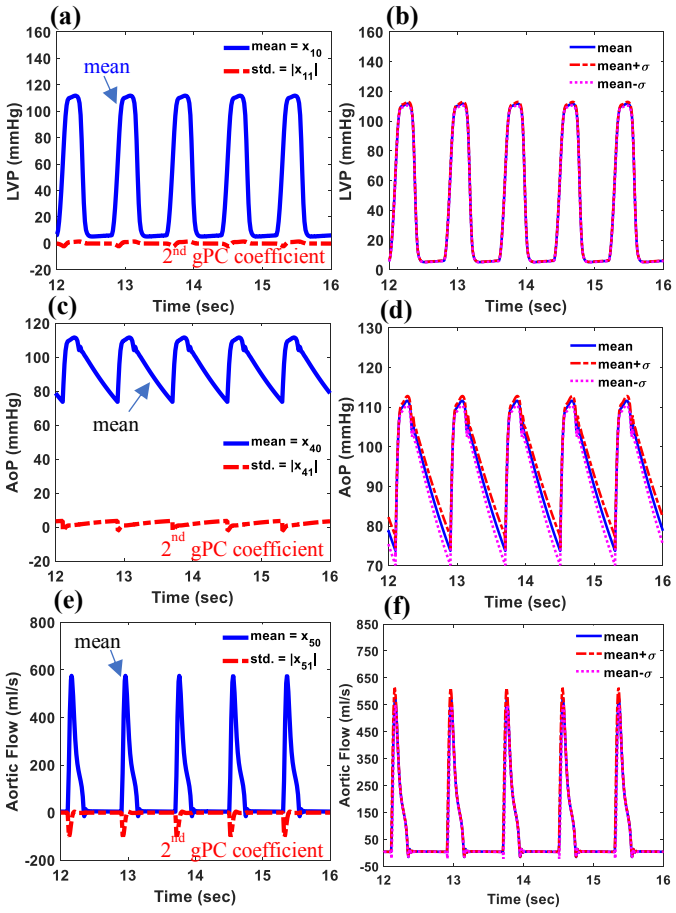

Figure 5. Simulated hemodynamic waveforms in the presence of uncertainty (the level of activity is set to1 mmHg/ml/s)

B. Constant Systemic Vascular Resistance

In this case study, it is assumed that the activity level of a patient has remained unchanged for a period of time. Thus, a constant R_s (SVR) value is used to show the controller can adjust the pump speed while avoiding suction. Specifically, R_s is set to 1 mm Hg/ml/s, for which the suction can happen if the pump speed $\omega(t)$ reaches about 1.6×10^4 rpm. Fig. 6 shows the controlled pump speed and the corresponding mean values of the pump flow. As seen, to meet the physiological demands, the controller can adjust and maintain the pump speed at a desired level without inducing suction. The speed stabilizes around 1.47×10^4 rpm. Note that, due to the limited space, only the noise-free simulations are shown in Fig. 6. The heart rate in this case study is 75 bpm, and the contractility strength of the native heart (E_{max}) is set to 2 mmHg/ml. The variation (uncertainty) in R_s is assumed to be normally distributed, i.e., a mean value of 1 mmHg/ml/s and a 10% change around the mean value. Since there is no sign change in the slope calculated from the minimum values of pump flow, the controller gain is fixed at c_1=0.76 in (14), i.e., the self-tuning procedure is not executed.

C. Time-varying Systemic Vascular Resistance

In the second case study, R_s changes over time in order to mimic changes in patient's physiological activities. The time-varying R_s can be mathematically defined as:

$$R_s = \begin{cases} 2 - t/10 & 0 \le t \le 10 \\ 1 & 10 \le t \le 30 \\ 1+(t-30)/10 & 30 \le t \le 40 \\ 2 & 40 \le t \le 55 \\ 2-(t-55)/10 & 55 \le t \le 65 \end{cases} \quad (15)$$

Note that only the mean values of R_s were used in (15) to define different levels of activity. As done in the first case study, the perturbations in R_s were assumed to be a 10% change around the corresponding mean values. The mean value of R_s was initially kept at 2 mm Hg/ml/s, then gradually decreased to 1 mm Hg/ml/s in 10 s and maintained at this level for 20 s. Starting from 30 s, R_s was increased to 2 mm Hg/ml/s in 10 s and maintained at this level for 15 s before decreased to 1 mmHg/ml/s again. The changes in R_s shows different levels of activities, e.g., the patient was initially resting (R_s=2) before started doing exercise such as walking (R_s=1). The response of the self-tuning controller is shown in Fig. 7.

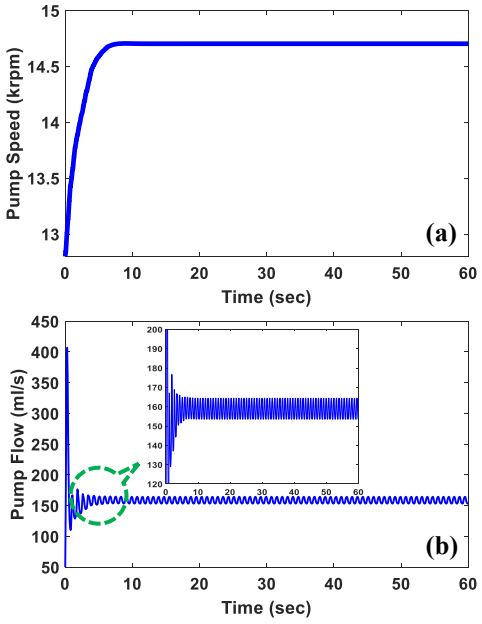

Figure 6. Simulations results of a constant level of activity. (a) controlled pump speed and (b) pump flow corresponding to the pump speed in (a)

As seen in Fig. 7 (a), the pump speed can be appropriately adjusted according to these dynamic changes in the activity. Such an adjustment can ensure sufficient cardiac outputs while preventing suction. Fig. 7 (b) shows the pump flow and the corresponding variance predicted at each time interval, which was used for the tuning of controller. Note that the controller gain in (14) was updated every 5 cardiac cycles to avoid any deleterious effect on the heart that might possibly result from the frequent change in the feedback controller. For comparison, a fixed controller gain without the self-tuning procedure was also used, and the simulation results are shown in Fig. 8. As compared to the self-tuning controller developed in this work, both controllers can adjust pump speeds to meet

physiological demands. However, it was found that the self-tuning controller has smaller excursions, as compared to the fixed controller (see Fig. 7 (a) and Fig. 8). Note that larger excursions in pump speed can possibly induce unsmooth and sudden changes in the pump flow, which can be harmful to the failing heart.

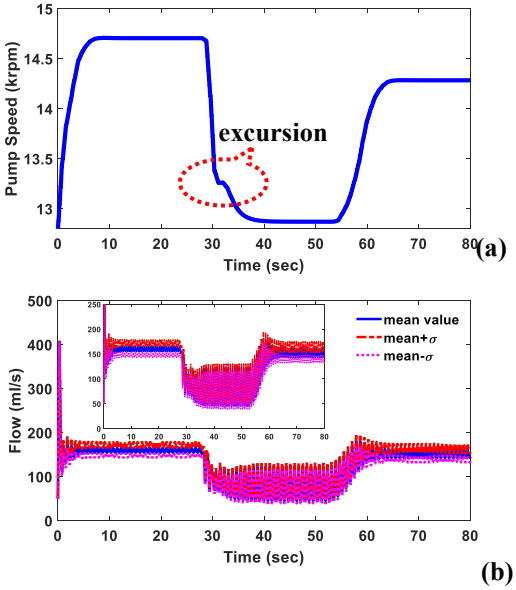

Figure 7. Sumulation resuts of a time-varying R_s which represents a sequence of changes in the level of activity. (a) controlled pump speed and (b) pump flow corresponding to the pump speed shown in (a)

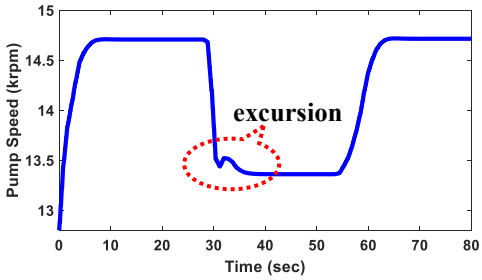

Figure 8. Simulation of a time-varying R_s with a fixed controller gain (c_1)

V. Conclusion

In this paper, a stochastic cardiovascular-pump model is developed by combining a previously reported model with a generalized polynomial chaos (gPC) expansion. Based on the gPC model, a self-tuning feedback controller is developed to adjust the pump speed to meet the physiological demands at different levels of physical activity, while taking the patient's variability into account. To show the efficiency of the new control algorithm, two case studies were investigated. It was found that the developed self-tuning controller can adjust the pump speed without inducing suction. As compared to a fixed controller gain, the self-tuning controller can provide better control performance. We would like to point out that different sources of uncertainty will be investigated in future work.

References

[1] N. Moazami, K. Fukamachi, M. Kobayashi, N. G. Smedira, K. J. Hoercher, A. L. S. Massiello, D. J. Horvath and R. C. Starling, "Axial and centrifugal continuous-flow rotary pumps: a translation from pump mechanics to clinical practice," *The Journal of Heart and Lung Transplantation,* vol. 32, no. 1, pp. 1-11, 2013.

[2] M. Simaan, A. Ferreira, S. Chen, J. Antaki and D. Galati, "A dynamical state state space representation and performance analysis of a feedback controlled rotary left ventricular assist device," *IEEE Transactions on Control Systems Technology,* vol. 17, no. 1, pp. 15-28, 2009.

[3] Y. Wang, S. Koenig, Z. Wu, M. Slaughter and G. Giridharan, "Sensorless physiologic control, suction prevention, and flow balancing algorithm for rotary biventricular assist devices," *IEEE Transactions on Control Systems Technology,* no. 99, pp. 1-15, 2017.

[4] Y. Wu, P. Allaire, G. Tao and D. Olsen, "Modeling, estimation, and control of human circulator system with a left ventricular assist device," *IEEE Transactions on Control Systems Tecnology,* vol. 15, no. 4, pp. 754-767, 2007.

[5] Y. Wang, S. Koenig, M. Slaughter and G. Giridharan, "Rotary blood pump control strategy for preventing left ventricular suction," *American Society for Artificial Internal Organs Journal,* vol. 61, no. 1, pp. 21-29, 2015.

[6] K. Ohuchi, D. Kikugawa, K. Takahashi, M. Uemura, M. Nakamura, T. Murakami, T. Sakamoto and S. Takatani, "Control strategy for rotary blood pumps," *Artificial Organs,* vol. 25, no. 5, pp. 366-370, 2005.

[7] A. Petrou, M. Kanakis, S. Boes, P. Pergantis, M. Meboldt and M. Daners, "Viscosity prediction in a physiologically controlled ventricular assist device," *IEEE Transactions on Biomedical Engineering,* vol. 65, no. 10, pp. 2355-2364, 2018.

[8] A. Siewnicka and K. Janiszowski, "A model for estimating the blood flow of the POLVAD pulsatile ventricular assist device," *IEEE Transactions on Biomedial Engineering,* p. in press, 2018.

[9] Y. Du, H. Budman and T. Duever, "Integration of fault diagnosis and control based on a trade-off between fault detectability and closed loop performance," *Journal of Process Control,* vol. 38, pp. 42-53, 2016.

[10] R. Hille and H. Budman, "Simultaneous identification and optimization of biochemical processes under model plant mismatch using output uncertainty bounds," *Computers & Chemical Engineering,* vol. 113, pp. 125-138, 2018.

[11] Z. Hu, D. Du and Y. Du, "Generalized polynominal chaos based uncertainty quantification and propagation in multiscale modeling of cardiac electrophysiology," *Computers in Biology and Medicine,* vol. 102, pp. 57-74, 2018.

[12] E. Lim, S. Dokos, S. Cloherty, R. Salamonsen, D. Mason, J. Reizes and N. Lovell, "Parameter optimized model of cardiovascular rotary blood pump interactions," *IEEE Transactions on Biomedical Engineering,* vol. 57, no. 2, pp. 254-266, 2010.

[13] G. Gridharan, M. Skliar, D. B. Olsen and G. M. Pantalos, "Modeling and control of a brushless DC axial flow ventricular assist device," *American Society for Artificial Internal Organs Journal,* vol. 48, pp. 272-289, 2002.

[14] H. Suga and K. Sagawa, "Instantaneous pressure volume relationships and their ratio in the excised, supported canine left ventricle," *Circulation Research,* vol. 35, no. 1, pp. 117-126, 1974.

[15] D. Xiu and G. E. Karniadakis, "The Wiener-Askey polynomial chaos for stochastic differential equations," *SIAM Journal on Scientific Computing,* vol. 24, no. 2, pp. 614-644, 2002.

[16] S. M. Kang, K. Her and S. W. Choi, "Outflow monitoring of a pneumatic ventricular assist device using external pressure sensors," *Biomedical Engineirng Online,* vol. 15, no. 1, pp. 100-122, 2016.

[17] C. Bartoli and R. Dowling, "The future of adult cardiac assist devices: novel systems and mechanical circulatory support strategies," *Cardiology Clinics,* vol. 29, no. 4, pp. 559-82, 2012.

[18] Y. Du, T. Duever and H. Budman, "Fault detection and diagnosis with parametric uncertainty using generalized polynomial chaos," *Computers and Chemical Engienering ,* vol. 76, pp. 63-75, 2015.